



Microstructures and mechanical properties of polylactic acid prepared by a cold rolling process



Lijun Wang, Jianhui Qiu*, Eiichi Sakai

Department of Machine Intelligence and Systems Engineering, Faculty of System Science and Technology, Akita Prefectural University, 84-4 Tsuchiya Ebinokuchi, Yurihonjo, Akita 015-0055, Japan

ARTICLE INFO

Article history:

Received 15 July 2015

Received in revised form 1 February 2016

Accepted 6 February 2016

Available online 8 February 2016

Keywords:

Polylactic acid

Rolling process

Microstructures

Mechanical properties

ABSTRACT

A cold rolling process was performed with extruded polylactic acid (PLA) as the crystalline polymer at different rolling ratios. The variations of the crystalline morphology, crystallinity, density, molecular orientation, and the microhardness were investigated during the process. Moreover, the dynamic mechanical properties and mechanical properties were evaluated by dynamic mechanical analysis and tensile test, respectively. The results showed that plastic deformation more easily occurred on the surface than on the interior. In addition, with the increase of the rolling ratio, the crystallinity decreased; however, the molecular orientation increased. Dynamic mechanical analysis revealed that the rolled PLA displayed an anisotropy during the process. Moreover, the tensile strength increased from 51.1 MPa to 86.0 MPa, and the fracture strain increased from 5.3% to 103.1%, in the case of a 60% rolling ratio along the rolling direction, indicating that the PLA was homogenized during the rolling process. This certified that an appropriate rolling process (i.e., the 60% rolling ratio) was conducive for improving the comprehensive mechanical properties of PLA in the rolling direction.

© 2016 Elsevier B.V. All rights reserved.

1. Introduction

In the field of materials, recycling is one of the most important technologies to conserve resources and to reduce waste. Biological degradation is widely considered as an effective recycling technology. In recent years, many biologically degradable polymers, e.g., polybutylene succinate (PBS), polycaprolactone (PCL) and polylactic acid (PLA) have been developed. Out of these polymers, PLA is considered as one of the most promising biodegradable, compostable, thermoplastic, and crystalline polymers. Additionally, PLA is a sustainable alternative to petrochemical-derived products and can be derived from renewable resources (Jonoobi et al., 2010). PLA has many advantages, such as high-strength, high-modulus (Garlotta, 2001) and good stiffness (Jonoobi et al., 2010). However, because PLA belongs to the group of brittle materials, the fracture strain is very low (approximately 5%) (Garlotta, 2001). Hence, this disadvantage may limit its applications in industry.

To improve the ductility of PLA and extend its industrial applications, many researchers have proposed various methods to increase its ductility while maintaining or reinforcing its original strength. To achieve ideal mechanical properties and to greatly enhance its

commercial potential, two common methods have been developed. One is to incorporate fillers into the polymers, such as calcium phosphate (Bleach et al., 2002), carbon nanotube (Kuan et al., 2008), and natural fibers (Oksman et al., 2003). In particular, Bondeson and Oksman (2007) prepared PLA/cellulose nanowhisker (PLA/CNW) nanocomposites, and the results of the tensile property tests showed that only relative small improvements in the tensile properties of the prepared nanocomposites were achieved (the tensile strength was 67.7 MPa, and the elongation at break was approximately 2.4%). Moreover, Jonoobi et al. (2010) reported that the tensile strength of cellulose nanofiber-reinforced PLA composites increased from 58 MPa to 71 MPa, whereas the maximum strain was only 2.7–3.4%.

The other approach is to prepare polymers by plastic processing. Carrasco et al. (2010) reported that extruded/injected PLA showed an increase in the elongation at break (32–35% higher). Rhim et al. (2006) found that PLA films prepared by the thermocompression method were strong and brittle, with maximum tensile strength and maximum elongation at break values of 44.0 ± 2.2 MPa and $3.0 \pm 0.1\%$, respectively. These researchers attempted to improve the mechanical properties of PLA by using plastic processing. Unfortunately, the effect was not as good as expected (Yu et al., 2008).

In general, it is well known that microstructures, including the crystalline structure, molecular orientation, and crystallinity, can influence the mechanical properties of crystalline polymers. Many

* Corresponding author. Tel.: +81 184 27 2134; fax: +81 184 27 2134.
E-mail address: qiu@akita-pu.ac.jp (J. Qiu).

researchers have reported that plastic processing, such as die-drawing (Chapleau et al., 2005), roller drawing (Lee et al., 2008), tensile drawing (Bao et al., 2012), equal channel angular extrusion (Qiu et al., 2012a), hydrostatic extrusion (Gibson et al., 1974) and rolling process (Qiu et al., 2012b), can achieve good mechanical properties. In particular, the rolling process can achieve high molecular orientation for polymers while preventing the generation of voids during processing, which has been reported by Nakayama et al. (2001). Therefore, the rolling process has been extensively employed for producing polymers with good properties, such as polyethylene (PE) (Wang et al., 1993), polyoxymethylene (POM) (Mohanraj et al., 2008), polypropylene (PP) (Qiu, 2002), and others. Both Qiu et al. (2000a) and Murata et al. (2013) investigated the changes of morphology and mechanical property in molded polymers. During plastic processing, a multilayer structure will form because of the different cooling processes on the surface as well as in the inner part (Murata et al., 2012). Moreover, the crystallinity is decreased and the molecular orientation is increased by the rolling process as observed with micro Fourier transform infrared (FT-IR) spectroscopy (Qiu et al., 2000b). These researchers obtained the internal structure information in the whole cross section of the polymer and accurately assessed the change of the PP microstructure via the rolling process. To the best of our knowledge, there has been no research conducted on the effect of crystallinity and orientation on microstructures (i.e., crystal morphology, crystallinity, and molecular orientation) and mechanical properties of PLA produced by a cold rolling process. Therefore, it is essential to know whether the rolling process changes the microstructure of PLA, which is key for improving of the mechanical properties of PLA, especially its ductility.

In the present work, a cold rolling process was carried out for extruded PLA as the crystalline polymer under different rolling ratios. The crystal morphology, crystallinity, and molecular orientation were investigated using optical microscopy (OPM), differential scanning calorimetry (DSC), density method, and X-ray diffraction (XRD). Moreover, the microhardness distribution, dynamic mechanical analysis, and tensile properties of PLA at each rolling ratio were measured. Based on the measurement results, the effects of the rolling ratios on the microstructures and mechanical properties were discussed.

2. Experimental

2.1. Materials

Poly(lactic acid) (PLA) was purchased from Nature Works LLC (Ingeo 3001D, America) with a density of 1.24 g/cm³ (ASTM D792) and a melt flow index of 22 g/(10 min) (ASTM D1238). Its residual moisture content was less than 0.025%, which was recommended to prevent viscosity degradation.

2.2. Specimen preparation and the rolling process

The basic PLA material was vacuum-dried at 50 °C for 8 h. Then, it was manufactured using a twin screw extruder (KZX25TW-60MG-NH (-1200)-AKT, Technovel Co., Ltd., Osaka, Japan) with a screw speed of 100 rpm, and the temperature profile was varied from 150 °C at the feeding zone to 190 °C at the die. The extruded PLA was cooled down in a water bath and pelletized after the first extrusion process. Then, the granular extruded PLA was dried at 50 °C for 8 h again, and PLA plates were produced by the same extruder at the same extrusion conditions. The reason for two extrusions is to compare the PLA and its composites with each other at the same thermal history and to discuss their properties in a later paper.

Thereafter, the extruded PLA plates were used for the rolling process. The rolling process was performed with different rolling ratios (0%, 20%, 40%, 60, and 75%) to evaluate the effect of the rolling ratio on the properties and morphology of PLA. 2000 mm (length) × 100 mm (width) × 1.2 mm (thickness; the maximum thickness was 1.6 mm) extruded plates were machined into specimens with dimensions of 100 mm (length) × 80 mm (width) × 1.2 mm (thickness; the maximum thickness was 1.6 mm). The rolling process was carried out by a rolling machine (TKE-0; Imoto Machinery Co., Ltd., Tokyo, Japan) at room temperature (23 ± 2 °C) with a rotation speed of 3 m/min (Fig. 1). The rolling direction was matched to the extrusion direction and the effective width and diameter of each roller were 150 mm and 100 mm, respectively. The rolling ratio ξ was calculated using the following equations.

$$\xi = \left[\frac{(H_0 - H_1)}{H_0} \right] \times 100\% \quad (1)$$

where H_0 is the initial thickness of the specimen, and H_1 is the thickness of the rolled specimen, which was measured by a micrometer after the rolling process.

Finally, the rolled plates were cut using a dumbbell-shaped mold to obtain specimens with dimensions of 75 mm (length) × 10 mm (width), but with different thicknesses based on the different rolling ratios. The different thicknesses of the rolled plates were achieved by adjusting the distance between the two rollers (Fig. 1). The specimens were used for evaluating the variations of crystallinity and molecular orientation of PLA and its mechanical properties.

2.3. Observation of internal microstructures

The internal microstructures of PLA with different rolling ratios were observed by a polarized optical microscopy (Eclipse model ME600D, NIKON, Tokyo, Japan) to investigate the variation of the crystal structures. To achieve visibility, the middle part of dumbbell-shaped specimens was cut into 10 μm slices in longitudinal sections by a microtome (RM2145, Leica Microsystems, Tokyo, Japan).

2.4. Investigation of crystallization behaviors

2.4.1. Differential scanning calorimetry

Differential scanning calorimetry (DSC) was performed using a DSC instrument (X-DSC7000, SII Nano Technology Inc., Tokyo, Japan). The specimens (approximately 10 mg) for the tests were cut from the middle part of the dumbbell-shaped specimens in the whole cross-sectional direction, and were scanned from 30 to 200 °C at a scan rate of 10 °C/min under a nitrogen flow of 50 mL/min. Only the heating process was carried out to investigate the effect of the rolling ratio on the crystallization behavior of the rolled PLA. The DSC result was obtained from three measurements of each specimen group. Again, the degree of crystallization χ_c of PLA was determined from the DSC heating traces by the following equation.

$$\chi_c = \left[\frac{\Delta H_m - \Delta H_c}{H_m^0} \right] \times 100\% \quad (2)$$

where ΔH_m is the melting enthalpy during the heating process, ΔH_c is the enthalpy of crystallization, ΔH_m^0 is the enthalpy for 100% crystallization of PLA, which is approximately 93.6 J/g (Kalb and Pennings, 1980).

2.4.2. Determination of the density

A water displacement method (JIS K7112, method A) was employed to measure the density of the rolled PLA by using an

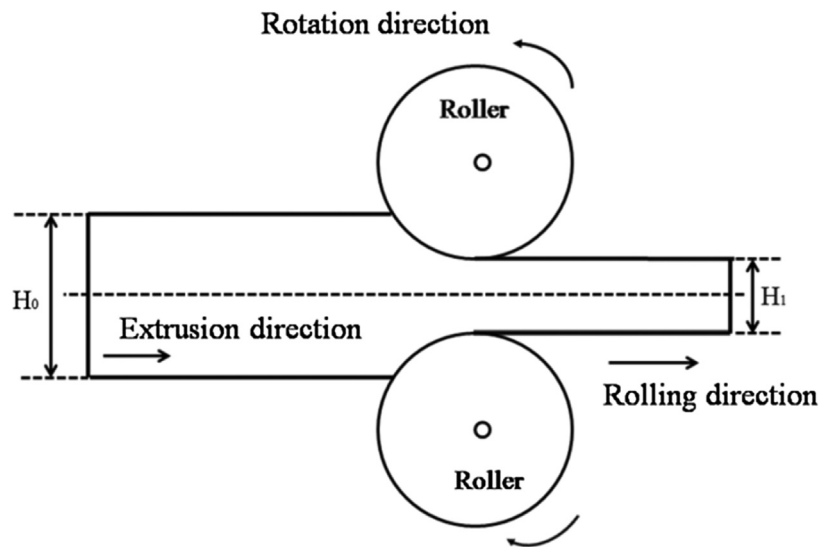


Fig. 1. Schematic of the rolling process.

electronic gravity meter (SD-200L, Alfa Mirage Co., Ltd., Osaka, Japan). The measurements were performed on the dumbbell-shaped specimens at room temperature ($23 \pm 2^\circ\text{C}$), and the water used was purified. The density of PLA was calculated by Eq. (3).

$$\rho = \frac{(m_{S,A} \times \rho_{IL})}{(m_{S,A} - m_{S,IL})} \quad (3)$$

where $m_{S,A}$ is the quality of PLA in the air, $m_{S,IL}$ is the quality of PLA in the water, and ρ_{IL} is the density of PLA in the water.

Moreover, the degree of crystallization χ_c of PLA was also determined by the density using the following equation.

$$\chi_c = \frac{(\rho - \rho_a)}{(\rho_c - \rho_a)} \times 100\% \quad (4)$$

where ρ is the measured density of PLA. The density of amorphous PLA (ρ_a) is 1.248 g/ml and the density of 100% crystalline PLA (ρ_c) is 1.290 g/ml, as reported by Nampoothiri et al. (2010) and Wei and Ma (2004).

2.5. Determination of the molecular orientation

The molecular orientation of the rolled PLA was determined by X-ray diffraction (XRD). The XRD patterns of PLA were recorded using Panalytical Xi Pert Pro (Cambridge, UK) with nickel-filtered Cu K α radiation ($\lambda=0.15418$ nm, XRD-6000, Shimadzu Co., Kyoto, Ltd.) operated at a generator voltage of 45 kV and a tube current of 40 mA. The specimen used was the dumbbell-shaped sample. The scattering angle was in the range of $2\theta=5\text{--}50^\circ$ at a scan speed of 2.13/min. To ensure accuracy and repeatability, XRD investigations of each specimen groups were repeated three times. The molecular orientation (H) was calculated by the following equation (Kakudo and Kasai, 1968):

$$H[\%] = \left[\frac{(180 - W)}{180} \right] \times 100\% \quad (5)$$

where W is the half-width of the diffraction peak.

2.6. Microhardness and its distribution

Microhardness measurements were performed using a manual turret microhardness tester (HNV-2000, Shimadzu Co., Ltd, Kyoto, Japan) to determine the surface microhardness and the microhardness distribution. The microhardness tester consisted of a computer

display and a Vickers square-based pyramidal diamond (with an angle of 136° between the opposite faces). The specimen used was the dumbbell-shaped specimen, and the microhardness distribution was determined by the microhardness of the middle part in the longitudinal sections (Fig. 2). The measurements were carried out with a load of 10 g for the recommended load-holding time of 15 s (JIS B 7774). Continuous measurements on the specimens were made at equally spaced ($50 \mu\text{m}$) points. The microhardness (H_V) was calculated with the following equation:

$$H_V = 0.189 \frac{P}{d^2} \quad (6)$$

where P is the force applied to the diamond (in kilograms-force) and d is the average length of the diagonal left by the indenter (in millimeters).

2.7. Dynamic Mechanical Analysis

Dynamic mechanical analysis was carried out with a dynamic mechanical analyzer (RSA-G2, TA Instruments, Wilmington, USA) in tension mode, and the storage modulus E' , loss modulus E'' , and $\tan \delta$ (δ is defined as the phase lag between the stress and the strain) were determined by the average value of three measurement results. The span of the girder was 20 mm. Strip test pieces were cut from the middle of the dumbbell-shaped specimen with a size of 30 mm (length) \times 5 mm (width). The test was performed in the temperature scan mode heating from 30 to 120°C at a programmed heating rate of $2^\circ\text{C}/\text{min}$. The amplitude of the strain was 0.1%, and the frequency was set at 1.0 Hz.

2.8. Tensile property tests

The tensile properties involving the tensile strength and the fracture strain of the PLA with different rolling ratios were measured using a universal testing machine (3360, INSTRON Co., Ltd., Kanagawa, Japan). The specimens used were the dumbbell-shaped specimens. The tests were carried out at a tensile rate of 10 mm/min under room temperature ($23 \pm 2^\circ\text{C}$). The values of the tensile properties of each group were determined from the means of five specimens.

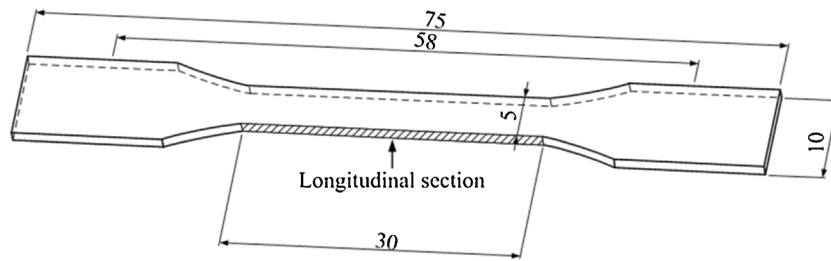


Fig. 2. Schematic diagram for the microhardness distribution test.

2.9. Scanning electron microscope

The microstructures of the fractured surfaces were observed by scanning electron microscopy (SEM, S-4300, Hitachi Ltd., Tokyo, Japan). The specimens were sputter-coated with gold using an ion sputtering apparatus (E-1030, Hitachi Science Systems Co., Ltd., Yokohama, Japan) to avoid charging. The acceleration voltage was 3 kV.

3. Results and discussions

3.1. Variation of the internal structure

It is well known that different plastic processes will lead to the formation of a multilayer and different microstructures between the surface and the interior of the obtained polymer products (Murata et al., 2012). Based on this view, the internal microstructures of unrolled and rolled PLA were investigated, and the morphologies are shown in Fig. 3.

Fig. 3(a) shows a micrograph near the surface of unrolled PLA, and it is obvious that the surface structure, as well as the structure of Fig. 3(b), showed a columnar microstructure. The size of the columnar microstructure was approximately 3–10 μm , while in the core layer, the size was approximately 5–12 μm , which was slightly larger than that of the surface. This may be because the surface layer was rapidly cooled, and only small-size microstructures were formed during the extrusion process. Yet in the core layer (Fig. 3(b)), columnar crystals with sizes of 5 μm can be clearly observed. These phenomena might have resulted because the surface of the specimen was subjected to forces from the extruder during the extrusion process and cooled rapidly in the air; thus, the crystals were small. The impact on the interior was very small, leading to the differences between the surface and the interior of the specimen. Moreover, for the PLA with a low rolling ratio (i.e., 20%, Fig. 3(c)), distinct changes in the microstructures of the interior were not observed compared to that of the unrolled PLA (Fig. 3(b)), but the microstructures were destroyed slightly and became smaller than before. Unexpectedly, for the specimens with high rolling ratios (i.e., $\xi = 40\%$, 60%, and 75%), the microstructures exhibited dramatic changes in the core layer. Most of the crystals were refined, but there were still unrefined parts, as shown in Fig. 3(g). In Fig. 3(d), columnar microstructures were mostly not observed, and the microstructures became very orderly. Furthermore, the size of these microstructures was smaller. This was because the surface of the specimen was subjected to a strong shear stress from the two rollers during the rolling process, resulting in the destruction of the original microstructures and crystal refinement; thus, the shape of the microstructures changed. A similar case can be observed in Fig. 3(e) and (f), which shows the microstructure near the surface and the microstructure of the core layer of 60% rolled PLA. Regardless of the surface vicinity and core layer, the size of the microstructures was smaller than that of the unrolled PLA. It was considered that the microstructures from the

surface to the core layer were completely refined under the high rolling ratio. Fig. 3(g) shows the heart part of the 60% rolled PLA, and it was found that there were still some large microstructures in the heart part (this case was similar to the 40% rolled PLA, which was omitted in this paper). However, the range of the large microstructures was small (approximately 60 μm). It was considered that the rolling ratio was not too high to be refined completely. Moreover, the microstructures were regularly arranged and orientated along the rolling direction. As the rolling ratio increased (Fig. 3(h)), the microstructures were further refined in the core layer. This phenomenon might be due to that PLA was a brittle polymer, and the original columnar microstructures were completely destroyed by a strong shear stress and were further refined under a high rolling ratio (i.e. $\xi = 75\%$).

In general, plastic deformation occurred more easily on the specimen surface which was in contact with the two rollers than in the core layer. The deformed layer was expanded as the rolling ratio increased. Furthermore, crystalline destruction and high molecular orientation occurred more easily in the case of high rolling ratios.

3.2. Effect of the rolling ratio on the crystallization behaviors

DSC measurements were carried out to investigate the effect of the rolling ratio on the crystallization behaviors of PLA, which was considered to influence its mechanical properties. Fig. 4 shows the DSC curves of PLA for various rolling ratios. All specimens exhibited three distinct peaks corresponding to the glass transition at approximately 60 $^{\circ}\text{C}$, cold crystallization at approximately 107–110 $^{\circ}\text{C}$, and melting at approximately 171–173 $^{\circ}\text{C}$. In other words, the thermal properties of the PLA were not distinctly changed during the rolling process. Moreover, it is interesting to note that there were double-melting peaks for the semi-crystalline PLA specimens after rolling at higher rolling ratios (e.g., $\xi = 40\%$, 60% and 75%). Double-melting peaks, which were related mainly to the cooling rate, have been reported previously (Yasuniwa et al., 2004).

The crystallization and melting behaviors of the PLA were examined, and the glass-transition temperature (T_g), cold crystallization temperatures (T_c), melting temperature (T_m), melting enthalpy (ΔH_m), crystallization enthalpy (ΔH_c), and the degree of crystallization (χ_c) were obtained, as tabulated in Table 1. Obviously, the T_g was basically maintained at approximately 59 $^{\circ}\text{C}$, and the T_m was slightly decreased with the increase of the rolling ratio. However, the T_c first increased and then decreased as the rolling ratio increased, which demonstrated that the rolling process was beneficial for the recrystallization of PLA up to a rolling ratio of 40%. Additionally, χ_c of PLA decreased with the increase of the rolling ratio (as shown in Fig. 5, and the maximum deviation of the crystallinity was approximately 3%). When the rolling ratio increased from 0% to 40%, χ_c decreased by 34.0%. Furthermore, as the rolling ratio was raised to 75%, χ_c dropped by approximately 61.7% to 1.8%. It can be inferred that the decrease of the crystallinity was due to crystalline deformation and crystals destruction, which led to the increase of plastic deformation during the rolling process. Similar

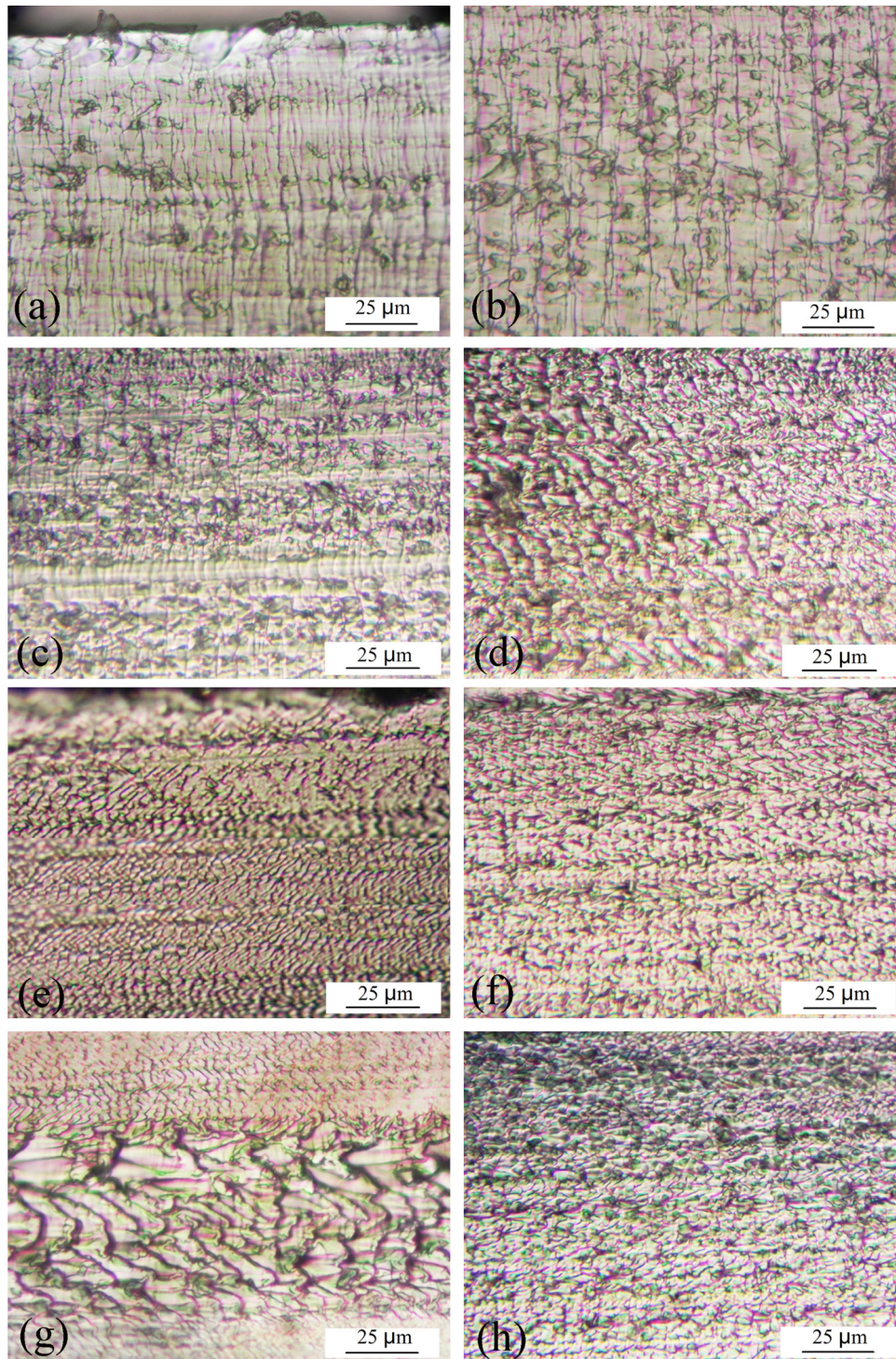


Fig. 3. Micrographs of PLA with different rolling ratios: (a) ξ : 0%, near the surface; (b) ξ : 0%, core layer; (c) ξ : 20%, core layer; (d) ξ : 40%, core layer; (e) ξ : 60%, near the surface; (f) ξ : 60%, core layer; (g) ξ : 60%, heart part, and (h) ξ : 75%, core layer.

Table 1

DSC data measured on unrolled and rolled PLA specimens.

Rolling ratio (%)	T_g (°C)	T_c (°C)	T_m (°C)	ΔH_m (mJ/mg)	ΔH_c (mJ/mg)	χ_c (%)
0	59.7	107.8	173.2	34.0	29.6	4.7
20	59.1	110.4	172.5	33.7	29.9	4.0
40	59.4	110.9	172.2	32.7	29.8	3.1
60	58.7	108.5	171.6	30.6	28.6	2.1
75	59.0	107.4	171.5	32.6	30.9	1.8

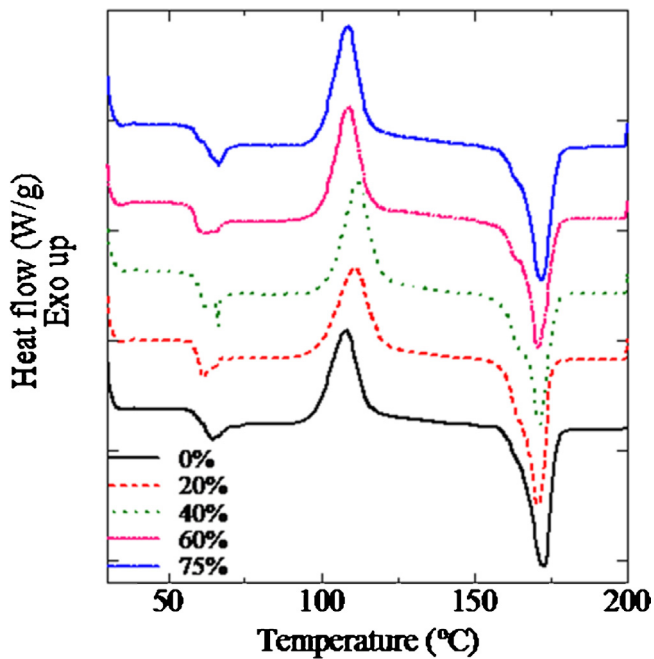


Fig. 4. DSC curves of unrolled and rolled PLA.

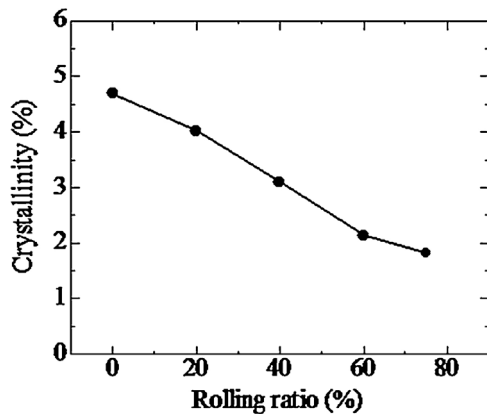


Fig. 5. Variation of the crystallinity of PLA as a function of the rolling ratio.

results were reported by Qiu and Jia for polypropylene (PP) using other evaluation methods (i.e., Fourier transform infrared spectroscopy (FT-IR) (Qiu et al., 2013) and X-ray diffraction (XRD) (Jia et al., 2008)). In addition, during the rolling process, the molecular chains may orientate highly in the amorphous phase, and the quasi-crystals were destroyed, which resulted in the decrease of χ_c .

To further confirm the aforementioned experimental results, the density method was utilized to measure the density of PLA, and then the variation of the PLA crystallinity was obtained. The density and crystallinity of the PLA as a function of the rolling ratio are shown in Fig. 6. The density of PLA decreased linearly with the increase of the rolling ratio from 1.2499 to 1.2487 at the rolling ratio of 75%, indicating a decrease of approximately 0.1%. Likewise, the degree of crystallinity decreased as the rolling ratio increased, which was in accord with the DSC results. The crystallization of unrolled PLA was 4.72%, but after being rolled by a 75% rolling ratio, the crystallinity suddenly dropped by 62.3% to 1.78%. This suggested that the crystallinity of PLA was relatively low, and the original crystals were destroyed during the rolling process; thus, the crystallinity decreased greatly. Similar results on other crystalline polymers (POM and PP) have been reported by

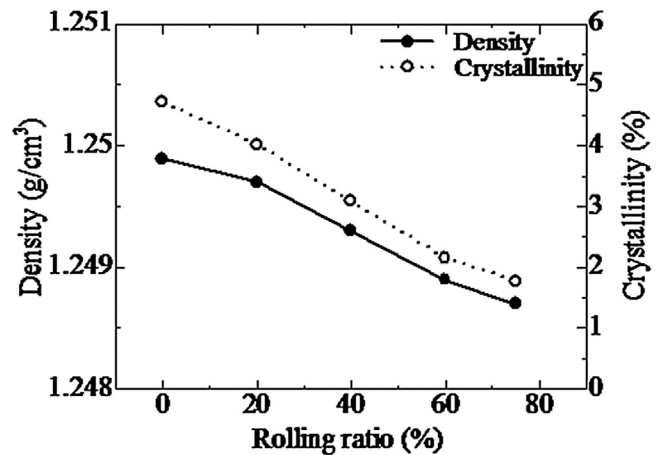


Fig. 6. Density and crystallinity of PLA as a function of the rolling ratio.

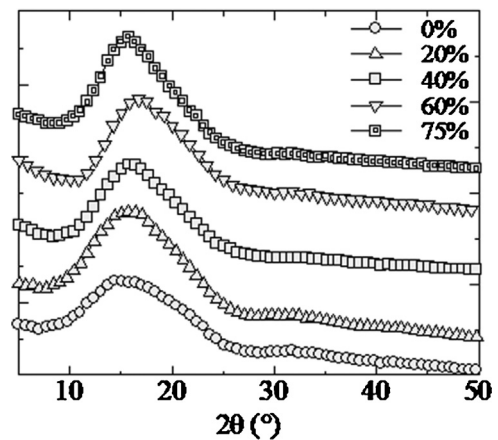


Fig. 7. XRD curves of PLA with different rolling ratios.

Pielichowski and Leszczynska (2005) and Qiu et al. (2000b), respectively.

3.3. Effect of the rolling ratio on the molecular orientation

XRD measurements were performed to evaluate the variation of the molecular orientation of PLA during the rolling process. Fig. 7 displays the XRD patterns in the range of $2\theta = 5^\circ - 50^\circ$. All specimens with different rolling ratios exhibited the most intense diffraction peak at $2\theta = 16.7^\circ$, corresponding to reflections from the (1 1 0) and (2 0 0) planes (Barrau et al., 2011), which belonged to the α -crystal form of PLA as reported previously (Marubayashi et al., 2012). Moreover, Fig. 7 shows that there were significant differences in the intensity, namely, the intensity of the diffraction peak at $2\theta = 16.7^\circ$, as the rolling ratios increased. The intensity of the diffraction peak represented the degree of order in the polymer, including the orientation and crystallization. Therefore, these results indicated that the rolling process did not change the crystal type, but significantly influenced the orientation of PLA. The variation of molecular orientation of PLA during the rolling process is shown in Fig. 8. It was obvious that the degree of molecular orientation increased as the rolling ratio increased. In particular, when the rolling ratio was less than 60%, the degree of molecular orientation increased linearly, but once the rolling ratio was beyond 60%, the increased degree became smaller. During the rolling process, the molecular chains were highly orientated in the amorphous phase, resulting in the increase of orientation. In other words, the rolling process contributed to the orientation of PLA in the amorphous phase.

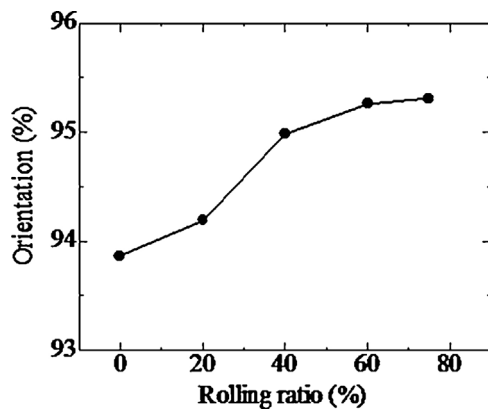


Fig. 8. Variation of the orientation of PLA as a function of the rolling ratio.

3.4. Microhardness and its distribution

Microhardness is related to the microstructures of crystal polymers in cross and longitudinal sections, such as the degree of molecular orientation, crystallinity, crystal size and crystal structure, as reported by Qiu (2005). The microhardness of the specimen surface and the microhardness distribution in the longitudinal sections were measured, and the results are shown in Fig. 9. Fig. 9(a) shows that the surface microhardness of unrolled PLA was approximately 18.5 kgf/mm², whereas as the rolling ratio increased, the microhardness decreased up to rolling ratio of 60%, and then a slight increase occurred. The results showed that the specimen was significantly softened after the rolling process, but when the rolling ratio reached 75%, the orientation was at the maximum (from the result of Fig. 8), and stress concentration was generated during the rolling process, leading to a slight increase in the microhardness of PLA.

Fig. 9(b) shows the microhardness distributions of the specimens with different rolling ratios in the longitudinal sections. The left side of the horizontal axis represents the specimen surface, and the right side represents the core. To make the relative position of the specimens of each layer (surface layer, intermediate layer, and core layer) consistent, the horizontal axis is the ratio of the distance from the surface and the half thickness. Overall, for the specimens with lower rolling ratios (i.e., $\xi = 0\%$ and 20%), the microhardness distributions could be divided into three regions from the surface to the core, i.e., a rise, a decline, and a plateau. In particular, for the unrolled PLA specimen, the microhardness of the intermediate layer was the largest, which was probably due to the extrusion process. It is well known that the intermediate layer was formed by rapid cooling and the impact of shear stress during the extrusion process. Therefore, the crystallinity and molecular orientation of the intermediate layer were higher, and the residual stress was greater, leading to a higher microhardness. However, in the case of the higher rolling ratios (i.e. $\xi = 40\%$, 60%, and 75%), the microhardness distribution integrally dropped, and the difference of the microhardness between each layer became more and more indistinct. This might be because the specimens were softened and became homogenized during the rolling process. Even for the 40% and 60% rolled specimens, although the heart part contained large microstructures, the microhardness of the specimens was not affected. In other words, an appropriate rolling ratio was necessary to produce a homogenized polymer, which perhaps improved the original mechanical properties of the polymer. Qiu (2001) also reported similar results on PP.

3.5. Dynamic mechanical behavior

The curves of the dynamic mechanical properties of rolled PLA are shown in Fig. 10. The storage modulus E' and $\tan \delta$ under different rolling ratios were clearly shown as a function of temperature. From Fig. 10, it can be found that at temperatures over 55 °C, E' sharply declined; the onset temperature was the glass transition temperature (T_g) of PLA. Overall, regardless of the rolling direction, E' decreased with the increase of temperature, but $\tan \delta$ showed an increasing trend. In Fig. 10 (a), in the region below the glass transition temperature, as the rolling ratio increased (i.e., $\xi = 20\%$, 40, 60%, and 75%), E' increased. In the high temperature region (e.g., 90 °C), E' was the same. For $\tan \delta$, in the region below the glass transition temperature, the values of rolled PLA were all higher than that of unrolled PLA, but in the high temperature region (e.g., 90 °C), the change of $\tan \delta$ was not significant. In Fig. 10(b), when the temperature was below the glass transition temperature, the variation trend of $\tan \delta$ was similar as that in Fig. 10 (a). However, in the high temperature region (e.g., 90 °C), the E' trend was somewhat different, i.e., little difference was observed in the E' of the specimens with different rolling ratios. This proved that the microstructures of PLA were changed by the rolling process, including the crystallinity, molecular orientation and so on; thus, PLA produced anisotropy during the rolling process. Moreover, as shown in both Fig. 10(a) and (b), E' exhibited a slight increase at 90 °C; this effect was due to cold crystallization at high temperatures (i.e., above 90 °C).

In addition, to discuss the effects of the rolling ratio on E' and $\tan \delta$ in detail, the data of Fig. 10 (E' and $\tan \delta$ at 30 °C) are plotted in Fig. 11. Comparing Fig. 11(a) and (b), it can be found that due to the different directions (parallel and vertical to the rolling direction), the trends of E' and $\tan \delta$ were different with each other. For the parallel direction (Fig. 11 (a)), E' dramatically increased with the increase of the rolling ratio and eventually reached a maximum value at a rolling ratio of 75%. E' was increased from 1.8 GPa to 3.3 GPa, i.e., an increase of 83%, compared to the unrolled PLA. However, the $\tan \delta$ of the 20% rolled PLA suddenly increased, and then the change of $\tan \delta$ was not obvious. In contrast, in the vertical direction (Fig. 11(b)), the change of E' was not obvious with an increase of the rolling ratio. Nevertheless, the effect of the rolling ratio on $\tan \delta$ was significant, especially in the case of the 20% rolling ratio. $\tan \delta$ increased by 3.1-fold from 2.0×10^{-2} to 8.1×10^{-2} and subsequently decreased linearly with the increase of the rolling ratio. Overall, regardless of the direction, i.e., parallel vs. vertical, when the rolling ratio was 20%, $\tan \delta$ was at a maximum. It was considered that PLA was softened during the rolling process, and the mobility of the molecules was enhanced, leading to the increase of $\tan \delta$.

3.6. Effect of rolling ratios on the tensile properties

To further prove that the variation of the internal microstructure during the rolling process, i.e., crystallinity and molecular orientation, would affect the mechanical properties of the polymers, tensile tests were carried out. The obtained results are shown in Fig. 12. Fig. 12(a) exhibits the nominal stress-strain curves of the PLA with various rolling ratios (i.e., $\xi = 0\%$, 40%, and 75%) parallel and vertical to the rolling direction. Obviously, the unrolled PLA was fractured within a strain of 10%, regardless of whether parallel or vertical to the rolling directions. However, after being rolled, the yield stress and tensile strength were significantly enhanced compared to the unrolled PLA, especially in the parallel direction; the strains were suddenly increased to more than 70% at the rolling ratio of 40%, showing a high ductility. It was proven that the large microstructures of the heart part could not affect the mechanical property of the rolled PLA. Moreover, the specimens with the rolling ratios of 40% or 75% had an even plastic deformation during

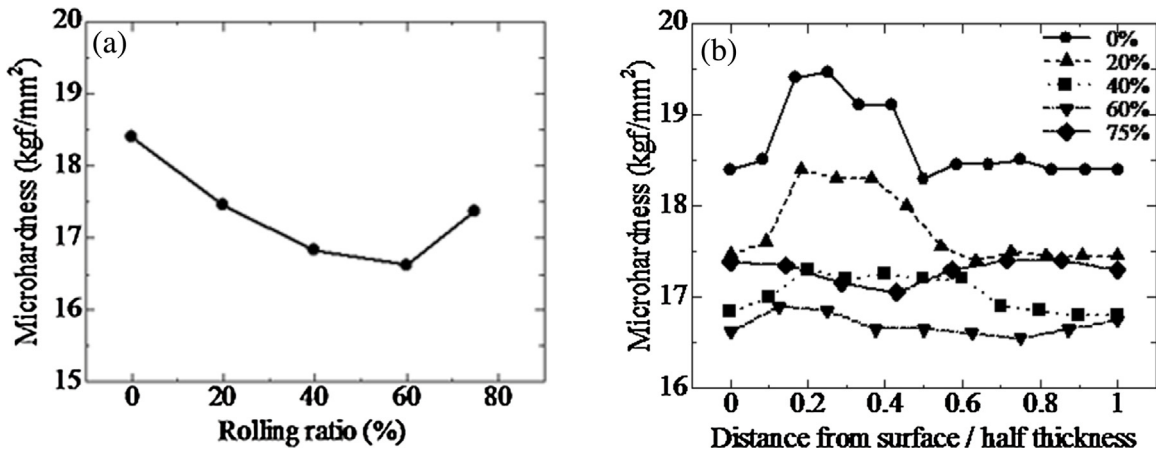


Fig. 9. Microhardness of PLA with different rolling ratios: (a) Surface microhardness and (b) microhardness distributions.

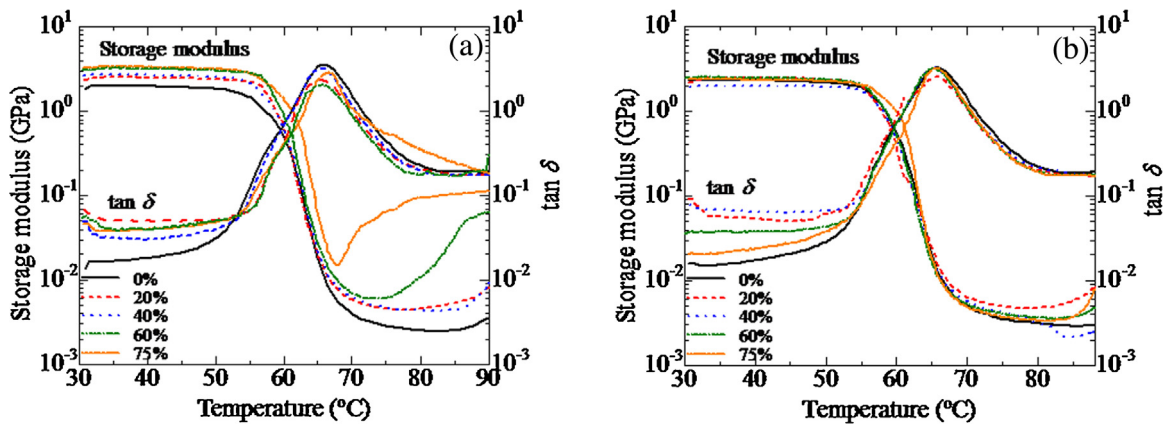


Fig. 10. Storage modulus and $\tan \delta$ of unrolled and rolled PLA: (a) Parallel to the rolling direction and (b) vertical to the rolling direction.

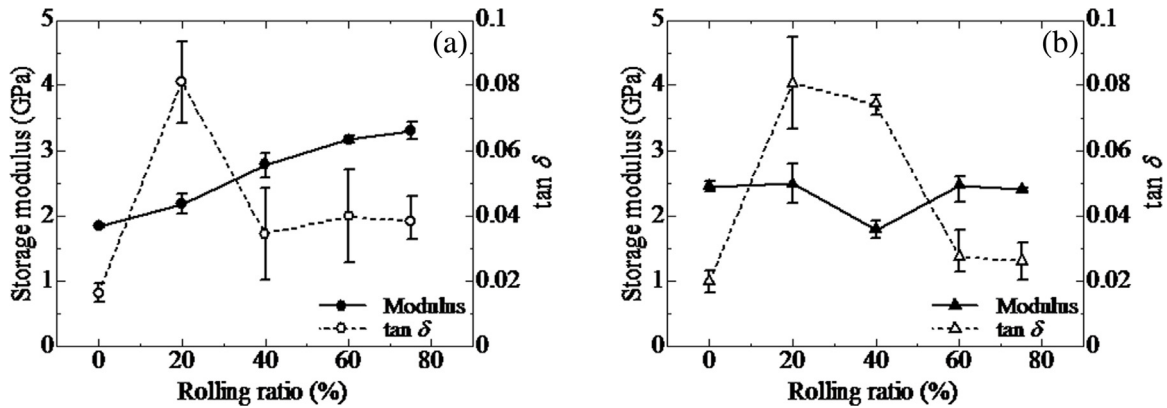


Fig. 11. Dynamic mechanical properties of the PLA at 30 °C: (a) Parallel to the rolling direction and (b) vertical to the rolling direction.

tensile testing; the middle of the specimens became thinner, and the transparency of the specimens increased. This result was consistent with the microhardness distribution in the longitudinal sections. It was confirmed that the internal microstructures of the specimens were greatly changed, and the PLA produced anisotropy during the rolling process, which coincided with the results of the dynamic mechanical analysis.

In Fig. 12(b), variations of the tensile strength and fracture strain are not obvious in the vertical direction. On the contrary, variations in the parallel direction were very notable; both the tensile strength and fracture strain were significantly increased with the increase of

the rolling ratio up to the 60%. When the rolling ratio reached 60%, the tensile strength and fracture strain increased from 51.1 MPa to 86.0 MPa and from 5.3% to 103.1%, respectively. It can be considered that the tensile property was anisotropic, thus having a different value when measured in different directions. This result was similar to the DMA results mentioned above. The reinforcement of the tensile properties was very striking despite the fact that they were decreased slightly at the rolling ratio of 75%. This was related to the microhardness distribution of PLA at the 75% rolling ratio, and the decreased tensile properties at the 75% rolling ratio can be eventually ascribed to the decrease of the molecular

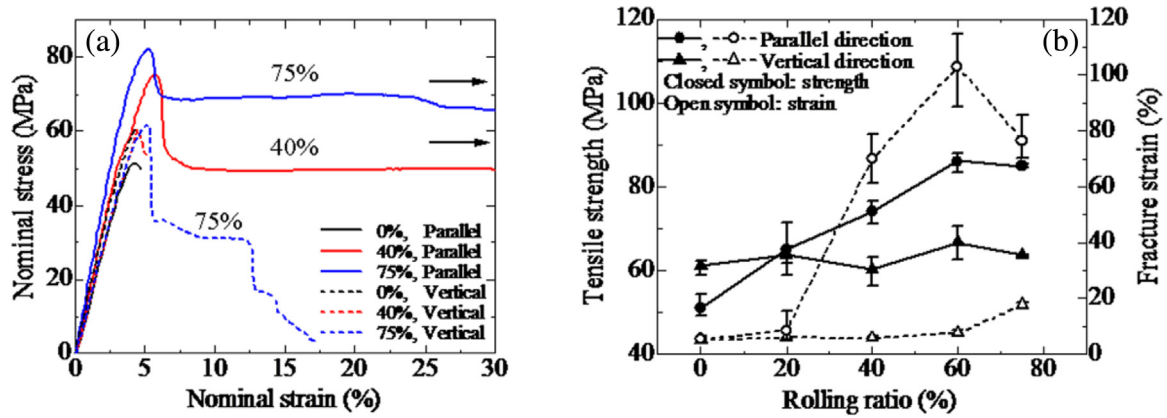


Fig. 12. Tensile properties of PLA: (a) Strain-stress curves and (b) tensile strength and fracture strain.

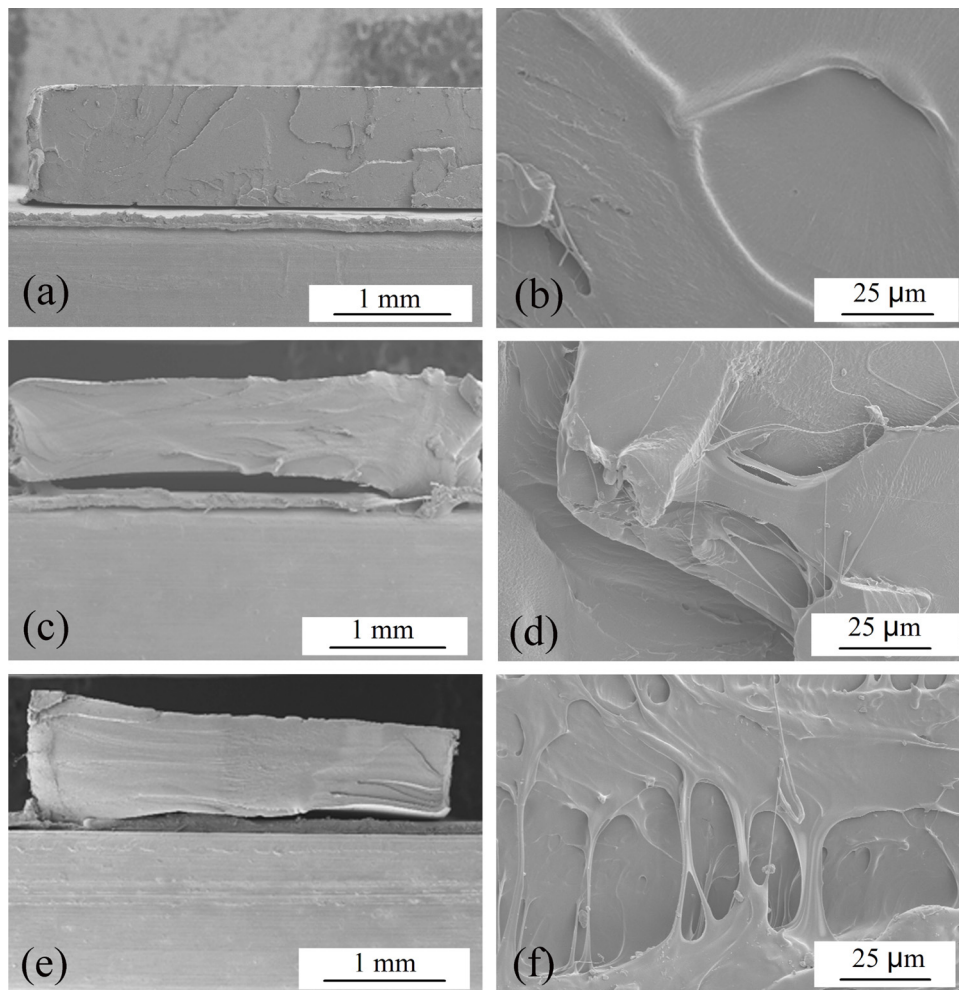


Fig. 13. SEM micrographs of tensile fractured surfaces: (a) ξ : 0%, (c) ξ : 40%, (e) ξ : 75%. (b), (d), and (f) are high-magnification micrographs of (a), (c) and (e), respectively.

orientation. Moreover, when the rolling ratio was 20%, the tensile strength of the parallel direction was the same as that of the vertical direction. This was one reason why the values of $\tan \delta$ of 20% rolled PLA were similar regardless of the direction in the DMA analysis (as shown in Fig. 11).

The data in Fig. 12 shows that the tensile properties of the rolled PLA in the parallel direction were affected by the rolling ratio greatly. Thus, the representative tensile fractured specimens were observed via SEM, and the SEM micrographs are shown in Fig. 13.

Fig. 13(a), (c), and (e) shows the whole fractured sections of the specimens with rolling ratios 0%, 40%, and 75%, respectively, and it was found that the starting points of the fractures appeared near the specimen surfaces. From Fig. 13(a), it can be clearly observed that the size of the fractured surfaces was not changed, and the high-magnification micrograph (Fig. 13(b)) shows that the interior of the fractured surface was smooth. Hence, a typical brittle fracture was observed. This phenomenon can be related to the microhardness distribution of the unrolled PLA as mentioned above. However,

Fig. 13(c) and (e) obviously shows that the fractured sizes of both specimens became smaller, indicating the typical characteristics of a ductile fracture. Due to the observation that the actual broken position was in the curved part of the specimen, the area of the fractured surface was larger than that of the parallel part. Furthermore, during the tensile test, a large amplitude recovery occurred in the specimen, resulting in the non-uniformity of the size of the fractured surface (as shown in Fig. 13 (e)). Moreover, from the high-magnification micrographs of the interiors (Fig. 13 (d) and (f)), it was observed that there were many fibrillar PLA on the fractured surfaces, especially in the case of the 75% rolling ratio (Fig. 13 (f)). The increase of the fracture toughness with rolling ratio can be related to the increase of fibril formation. Although the surface crystals of PLA were destroyed during the rolling process, they were highly orientated in the interior along the rolling direction. Additionally, based on the microhardness distribution from previously, the PLA specimens were homogenized at a high rolling ratio; thus, the tensile properties of rolled PLA were reinforced.

The microhardness distribution of the rolled PLA with a high rolling ratio exhibited homogenization. The microhardness of the intermediate layer became lower during the rolling process, leading to smaller differences between the mechanical reactivity and the surrounding; thus, the local stress concentration was eased, and the specimens were not prone to cracking, resulting in the improvement of strength and the increase in the ductility of the PLA.

4. Conclusion

The present work demonstrated the effect of rolling conditions on the microstructures and mechanical properties of PLA in a cold rolling process, which is an industrially relevant plastic processing technique for large-scale production. The crystal morphology, crystallinity, molecular orientation, and mechanical properties of the rolled PLA were investigated in detail. Based on the results obtained, the most important factors influencing the plastic processing of PLA for industrial applications are listed below.

1. Plastic deformation occurred more easily on the surface than in the interior of the PLA. The deformation layer expanded with the increase of the rolling ratio. Moreover, at a high rolling ratio, crystalline destruction and high molecular orientation occurred in the core layer of the rolled PLA.
2. The rolling process did not influence the thermal properties of the PLA. However, the crystallinity of PLA decreased as the rolling ratio increased.
3. The rolling process did not change the crystal type of PLA and contributed to the increase of the PLA orientation degree.
4. The microhardness distributions of the PLA with lower rolling ratios were divided into three regions, i.e., a rise, a decline, and a plateau. An appropriate rolling ratio (e.g., $\xi = 40\%$ and 60%) was necessary to produce a homogenized polymer, which could improve the original mechanical properties of the PLA.
5. The dynamic mechanical properties showed that the PLA was softened and produced an anisotropy during the rolling process. In particular, at a temperature of 30°C , the $\tan \delta$ of the parallel direction showed an increasing trend. This indicated that the mobility of molecules was enhanced during the rolling process.
6. When the rolling ratio reached 60% , the tensile strength and fracture strain in the rolling direction increased from 51.1 MPa to 86.0 MPa and from 5.3% to 103.1% , respectively. The ductility of PLA was greatly improved. Moreover, the tensile properties of the rolled PLA in the rolling direction were mostly reinforced compared with that in the vertical direction, due to the high molecular orientation along the rolling direction.

References

- Bao, R., Ding, Z., Zhong, G., Yang, W., Xie, B., Yang, M., 2012. Deformation-induced morphology evolution during uniaxial stretching of isotactic polypropylene: effect of temperature. *Colloid Polym. Sci.* 290, 261–274.
- Barrau, S., Vanmansart, C., Moreau, M., Addad, A., Stoclet, G., Lefebvre, J.M., Seguela, R., 2011. Crystallization behavior of carbon nanotube–poly(lactide) nanocomposites. *Macromolecules* 44, 6496–6502.
- Bleach, N.C., Nazhat, S.N., Tanner, K.E., Kellomäki, M., Törmälä, P., 2002. Effect of filler content on mechanical and dynamic mechanical properties of particulate biphasic calcium phosphate poly(lactide) composites. *Biomaterials* 23, 1579–1585.
- Bondeson, D., Oksman, K., 2007. Poly(lactide) acid/cellulose whisker nanocomposites modified by poly(vinyl alcohol). *Compos. Part A: Appl. Sci. Manuf.* 38, 2486–2492.
- Carrasco, F., Pagès, P., Gámez-Pérez, J., Santana, O.O., MasPOCH, M.L., 2010. Processing of poly(lactide acid) Characterization of chemical structure, thermal stability and mechanical properties. *Polym. Degrad. Stab.* 95, 116–125.
- Chapleau, N., Mohanraj, J., Aji, A., Ward, I.M., 2005. Roll-drawing and die-drawing of toughened poly(ethylene terephthalate) Part 1. Structure and mechanical characterization. *Polymer* 46, 1956–1966.
- Garlotta, D., 2001. A literature review of poly(lactide acid). *J. Polym. Environ.* 9, 63–84.
- Gibson, A.G., Ward, I.M., Cole, B.N., Parsons, B., 1974. Hydrostatic extrusion of linear polyethylene. *J. Mater. Sci.* 9, 1193–1196.
- Jia, J., Mao, W., Raabe, D., 2008. Changes of crystallinity and spherulite morphology in isotactic polypropylene after rolling and heat treatment. *J. Univ. Sci. Technol. Beijing Mineral Metall. Mater.* 15, 514–520.
- Jonoobi, M., Harun, J., Mathew, A.P., Oksman, K., 2010. Mechanical properties of cellulose nanofiber (CNF) reinforced poly(lactide acid) (PLA) prepared by twin screw extrusion. *Compos. Sci. Technol.* 70, 1742–1747.
- Kakudo, M., Kasai, N., 1968. X-ray Diffraction by Macromolecules. Maruzen, Japan, pp. 187–200.
- Kalb, B., Pennings, A.J., 1980. General crystallization behavior of poly(L-lactide acid). *Polymer* 21, 607–612.
- Kuan, C.F., Kuan, H.C., Ma, C.C.M., Chen, C.H., 2008. Mechanical and electrical properties of multi-wall carbon nanotube/poly(lactide acid) composites. *J. Phys. Chem. Solids* 69, 1395–1398.
- Lee, S.H., Nakayama, K., Cho, H.H., 2008. Fine structure and physical properties of poly(butylene terephthalate) sheets prepared by roller drawing method. *Fiber Polym.* 9, 740–746.
- Marubayashi, H., Asai, S., Sumita, M., 2012. Complex crystal formation of poly(L-lactide) with solvent molecules. *Macromolecules* 45, 1384–1397.
- Mohanraj, J., Morawiec, J., Pawlak, A., Barton, D.C., Galeski, A., Ward, I.M., 2008. Orientation of polyoxymethylene by rolling with side constraints. *Polymer* 49, 303–316.
- Murata, T., Qiu, J.H., Sakai, E., Wu, X., Kudo, M., 2012. Morphology Change of extrusion molded crystalline polymer by rolling process. *Adv. Mater. Res.* 391–392, 595–599.
- Murata, T., Qiu, J.H., Wu, X., 2013. Effect of rolling temperature on microstructure and tensile properties of polypropylene. *Polym. Eng. Sci.* 53, 2573–2581.
- Nakayama, K., Qi, K., Hu, X., 2001. Dynamic mechanical properties of rolled polypropylene sheets. *Polym. Compos.* 9, 151–156.
- Nampoothiri, K.M., Nair, N.R., John, R.P., 2010. An overview of the recent developments in poly(lactide) (PLA) research. *Bioresour. Technol.* 101, 8493–8501.
- Oksman, K., Skrifvars, M., Selin, J.F., 2003. Natural fibres as reinforcement in poly(lactide acid) (PLA) composites. *Compos. Sci. Technol.* 63, 1317–1324.
- Pielichowski, K., Leszczynska, A., 2005. Structure-property relationships in polyoxymethylene/thermoplastic polyurethane elastomer blends. *J. Polym. Eng.* 25, 359–373.
- Qiu, J., 2001. Microstructure and tensile property of cold rolled PP/LCP blends. *Trans. Jpn. Soc. Mech. Eng.* A 67, 1458–1463.
- Qiu, J., 2002. Effect of the stress amplitude and the test temperature on the fatigue property of cold rolled PP. *Trans. Jpn. Soc. Mech. Eng.* A 68, 65–73.
- Qiu, J., 2005. Effects of flow distance and injection speed on the fatigue property of injection-molded polypropylene sheets. *Kobunshi Ronbunshu* 62, 425–431.
- Qiu, J., Kawagoe, M., Mizuno, W., Morita, M., 2000a. Effect on fatigue failure of injection-molded polypropylene sheets by rolling process. *Kobunshi Ronbunshu* 57, 255–262.
- Qiu, J., Kawagoe, M., Mizuno, W., Morita, M., 2000b. Effect of morphology and tensile properties of polypropylene by the rolling process. *Trans. Jpn. Soc. Mech. Eng.* A 66, 867–874.
- Qiu, J., Murata, T., Wu, X., Kitagawa, M., Kudo, M., 2012a. Plastic deformation mechanism of crystalline polymer materials in the equal channel angular extrusion process. *J. Mater. Process. Tech.* 212, 1528–1536.
- Qiu, J., Murata, T., Takahashi, K., Wu, X., 2012b. The plastic deformation characteristics of crystalline polymer materials via rolling process. *Adv. Mater. Res.* 391–392, 585–589.
- Qiu, J., Murata, T., Wu, X., Kudo, M., Sakai, E., 2013. Plastic deformation mechanism of crystalline polymer materials during the rolling process. *J. Mater. Sci.* 48, 1920–1931.
- Rhim, J.W., Mohanty, A.K., Singh, S.P., Ng, P.K.W., 2006. Effect of the processing methods on the performance of poly(lactide) films: thermocompression versus solvent casting. *J. Appl. Polym. Sci.* 101, 3736–3742.

Wang, M.D., Nakanishi, E., Hibi, S., 1993. [Effect of molecular weight on rolled high density polyethylene: 1. Structure: morphology and anisotropic mechanical behaviour](#). *Polymer* 34, 2783–2791.

Wei, G., Ma, P.X., 2004. [Structure and properties of nano-hydroxyapatite/polymer composite scaffolds for bone tissue engineering](#). *Biomaterials* 25, 4749–4757.

Yu, L., Liu, H., Xie, F., Chen, L., Li, X., 2008. [Effect of annealing and orientation on microstructures and mechanical properties of polylactic acid](#). *Polym. Eng. Sci.* 48, 634–641.

Yasuniwa, M., Tsubakihara, S., Sugimoto, Y., Nakafuku, C., 2004. [Thermal analysis of the double-melting behavior of poly\(L-lactic acid\)](#). *J. Polym. Sci. Polym. Phys.* 42, 25–31.